Time-domain implementation of an impedance boundary condition with boundary layer correction
Supplementary material

E.J. Brambley[a,*], G. Gabard[b]

[a]*Department of Applied Mathematics and Theoretical Physics, University of Cambridge, Wilberforce Road, Cambridge, CB3 0WA, United Kingdom*
[b]*Institute of Sound and Vibration Research, University of Southampton, Highfield, Southampton, SO17 1BJ, United Kingdom*

1. Validation of the Discrete Dispersion Analysis

In section 3.2 of the main paper, the time-domain numerical solutions of the linearized Euler equation are compared with a Discrete Dispersion Analysis [19] of the time-domain numerics, with the continuous analytic solution [39] as a reference. An example of the agreement between the time-domain numerics and the DDA is shown in figure 6 of the main paper, and it is claimed that the excellent agreement seen is typical. This allows the DDA results to be used for the remainder of the paper, with their better resolution at lower growthrates owing to a lack of numerical rounding errors. Here, further evidence is provided of the good agreement between time-domain numerics and the DDA, even in situations where the numerics fail to correctly reproduce the underlying analytic continuous solution (labelled Modified BC).

Figure 1 shows good agreement between time-domain numerics and the DDA when the grid spacing used leads to under-resolution. The parameters for figure 1 are those used for figure 7(b) of the main paper in the case $\Delta x = 0.01$.

Figure 2 similarly shows good agreement between the time-domain numerics and the DDA for an unfiltered case with a huge numerical instability very close to the Nyquist frequency. This case corresponds to the curve labelled "Characteristic" in figure 8 of the main paper.

Figure 3 shows good agreement between the time-domain numerics and the DDA when the boundary condition is applied either directly or using the method of characteristics. This plot is the equivalent of the "Direct Filtered" and "Characteristic Filtered" curves in figure 8 of the main paper.

Finally, figure 4 shows good agreement between the time-domain numerics and the DDA for the various filtering techniques used to plot figure 11 of the main paper.

In particular, it is clear from figure 4 that the DDA, as well as accurately representing the behaviour of the time-domain numerics, is able to resolve secondary instabilities (such as those occurring around $k \approx 600$) which Fourier transforms of the time-domain numerics are unable to resolve accurately due to rounding errors; the secondary instability is only captured by the time-domain numerics in figure 4(b), but is seen from the DDA to also be present in figures 4(a) and 4(c). This is the reason the DDA results are used for the later figures in the main paper.

*Corresponding author. Tel.: +44 1223 760457. Fax.: +44 1223 765900.
Email addresses: E.J.Brambley@damtp.cam.ac.uk (E.J. Brambley), gabard@southampton.ac.uk (G. Gabard)

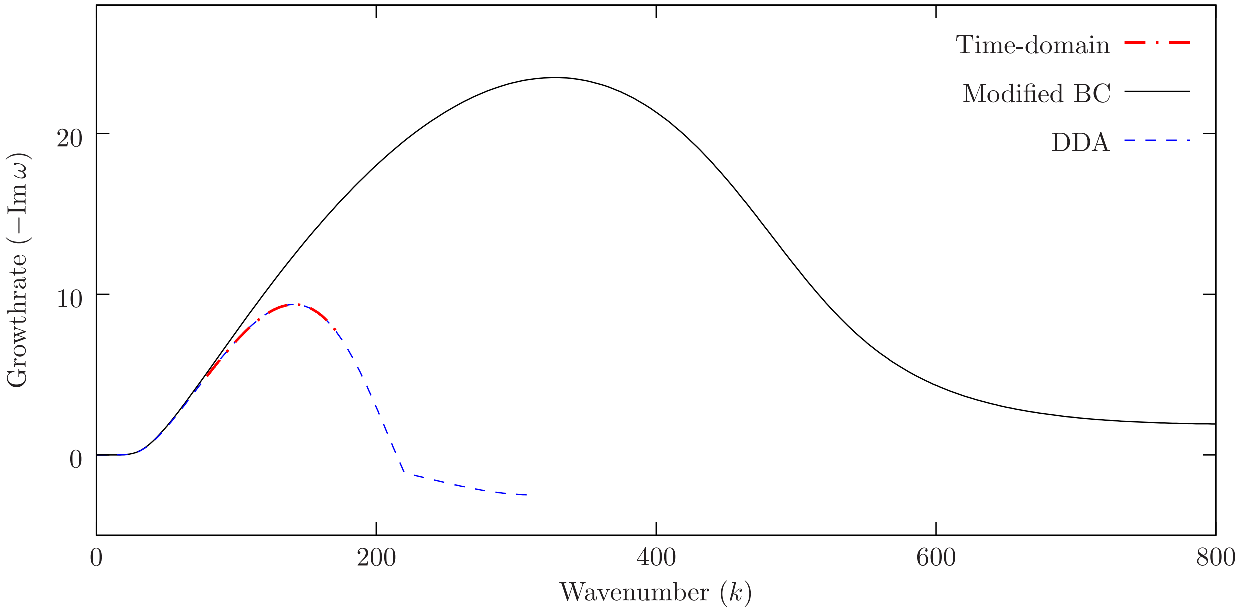

Figure 1: Exponential growth rate as a function of wavenumber for case B, grid 1, applying the boundary condition using characteristics, with the incoming characteristic filtered using the n7 filter. The time-domain computational result is obtained from a discrete Fourier transform of the growth between times $t = 4.5$ and $t = 5.7$.

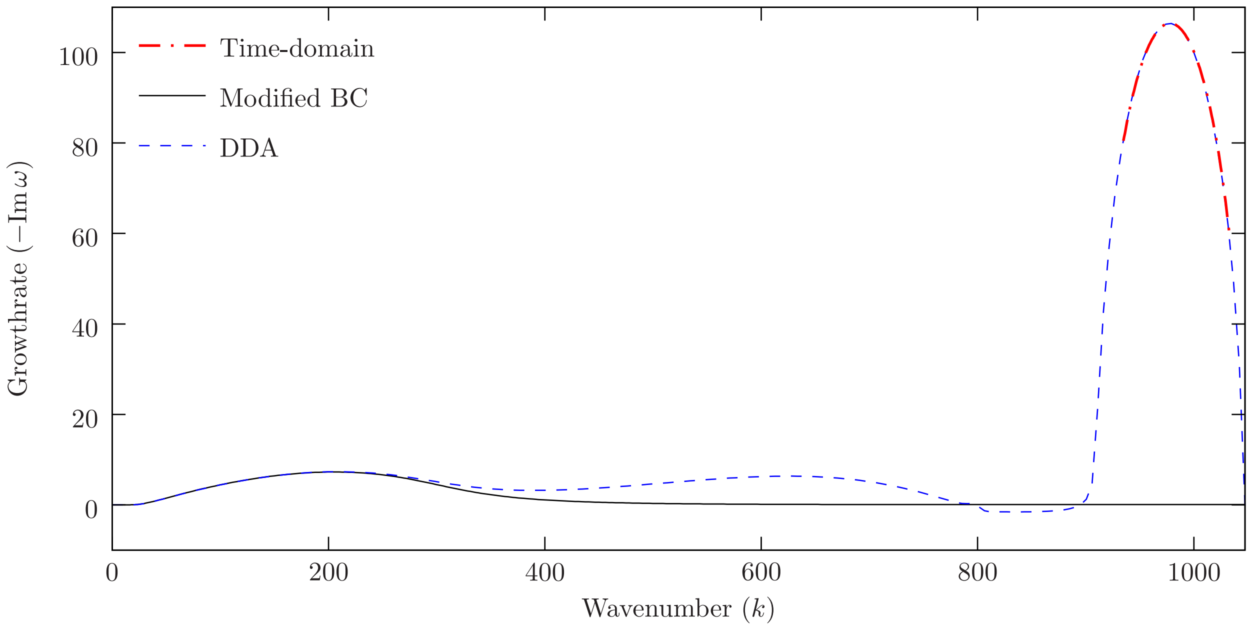

Figure 2: Exponential growth rate as a function of wavenumber for case C, grid 3, applying the boundary condition using characteristics with no filtering. The time-domain computational result is obtained from a discrete Fourier transform of the growth between times $t = 0.5$ and $t = 1.0$.

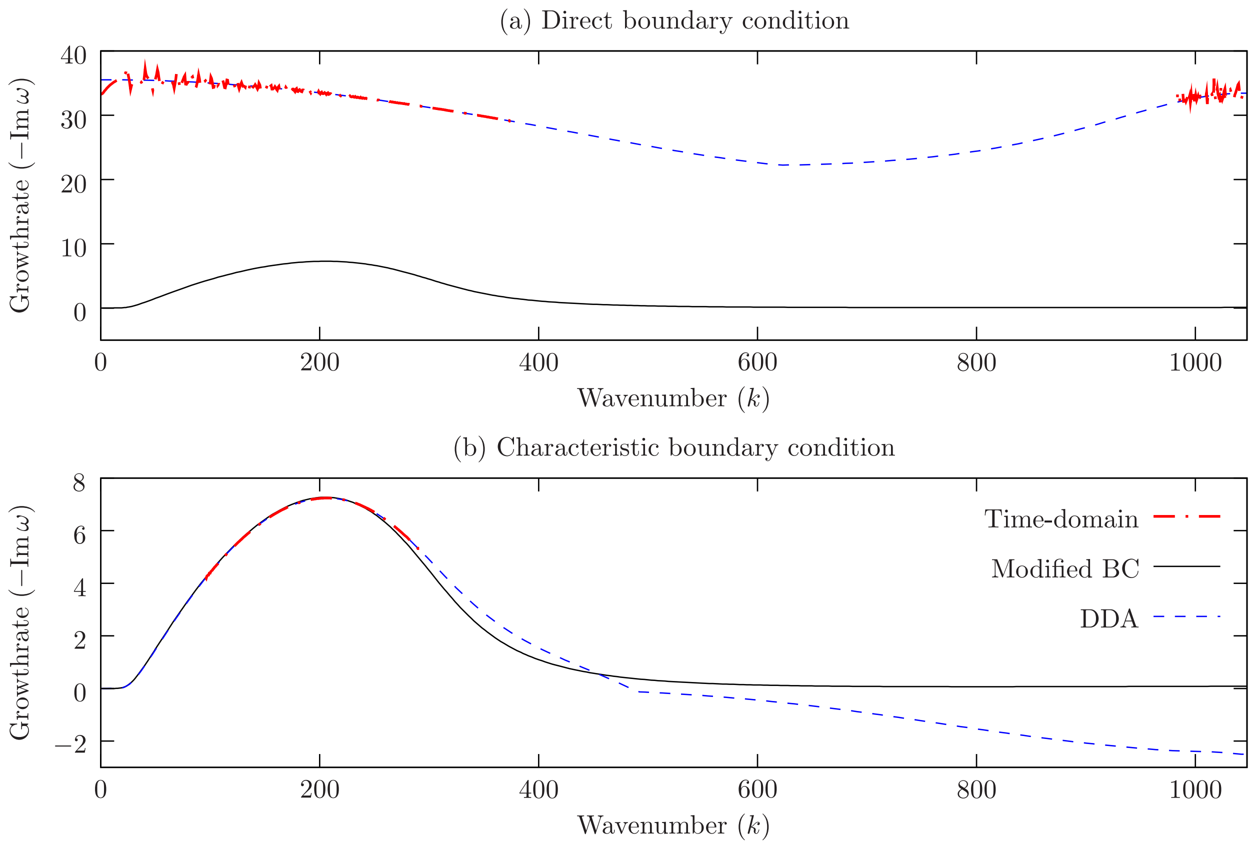

Figure 3: Exponential growth rate as a function of wavenumber for case C, grid 3, applying the boundary condition using either the direct (a) or characteristic (b) methods, both using the n7 filtering. The time-domain computational result is obtained from a discrete Fourier transform of the growth between times $t = 3.2$ and $t = 4.5$ (a), and $t = 7.2$ and $t = 10.6$ (b).

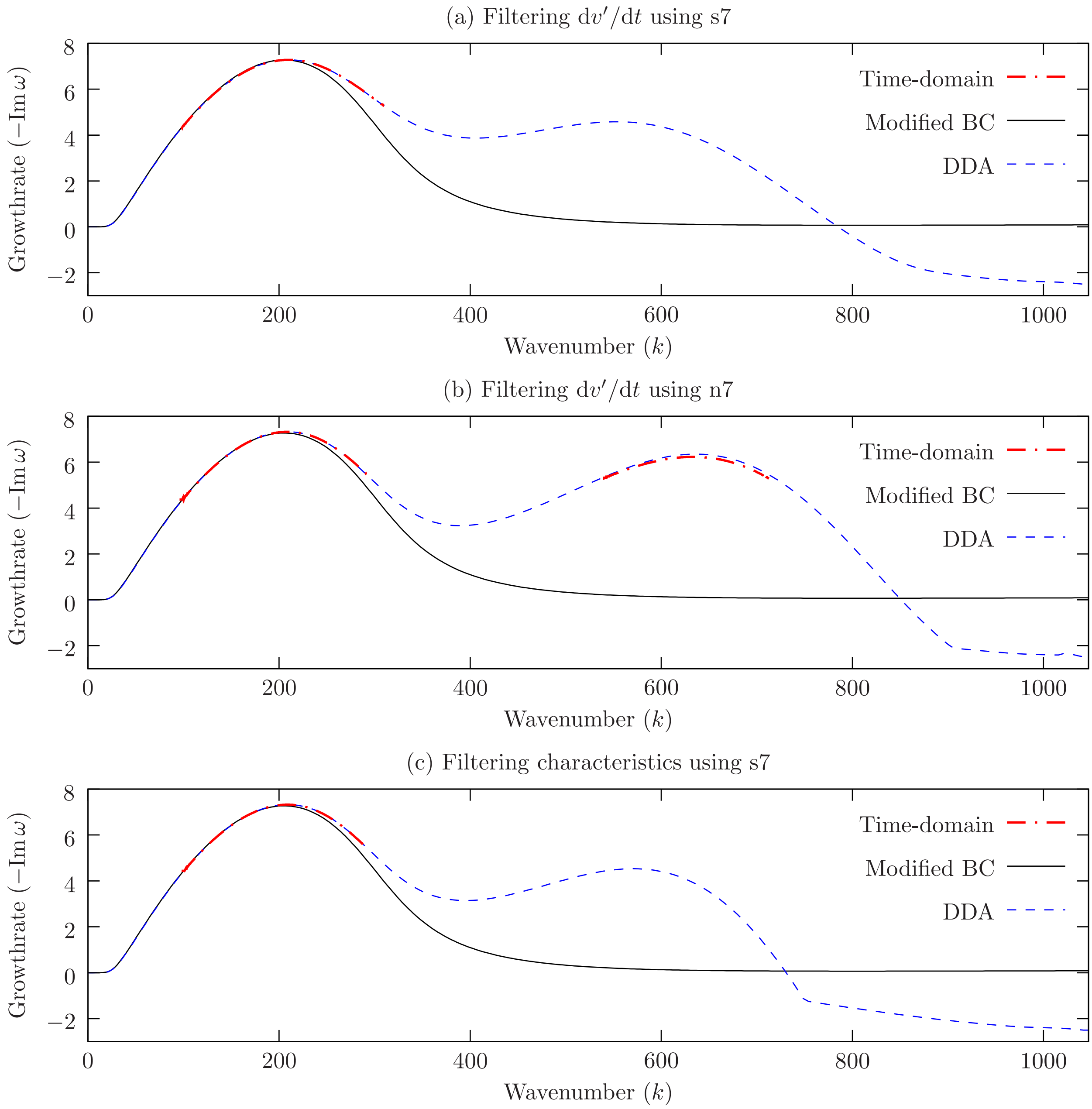

Figure 4: Exponential growth rate as a function of wavenumber for case C, grid 3, applying the boundary condition using the characteristic method, and filtering either the characteristic or $\mathrm{d}v'/\mathrm{d}t$ using the s7 or n7 filters. The time-domain computational result is obtained from a discrete Fourier transform of the growth between times $t = 7.2$ and $t = 10.6$.